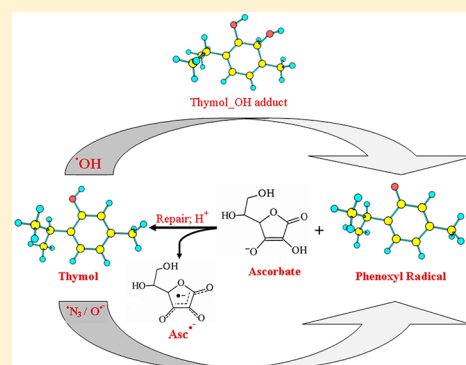


Oxidation Reactions of Thymol: A Pulse Radiolysis and Theoretical Study

S. Venu,[†] D. B. Naik,[‡] S. K. Sarkar,[‡] Usha K. Aravind,[§] A. Nijamudheen,^{||,&} and C. T. Aravindakumar^{*,†,‡,#}[†]School of Chemical Sciences, [§]Advanced Centre of Environmental Studies and Sustainable Development, [‡]School of Environmental Sciences, and [#]Inter University Instrumentation Centre, Mahatma Gandhi University, Kottayam 686560, Kerala, India[‡]Radiation and Photochemistry Division, Bhabha Atomic Research Centre, Mumbai 400085, India^{||}Indian Institute of Science Education and Research, Thiruvananthapuram, Kerala, India

S Supporting Information

ABSTRACT: The reactions of $\bullet\text{OH}$ and $\text{O}^{\bullet-}$, with thymol, a monoterpene phenol and an antioxidant, were studied by pulse radiolysis technique and DFT calculations at B3LYP/6-31+G(d,p) level of theory. Thymol was found to efficiently scavenge OH radicals ($k = 8.1 \times 10^9 \text{ dm}^3 \text{ mol}^{-1} \text{ s}^{-1}$) to produce reducing adduct radicals, with an absorption maximum at 330 nm and oxidizing phenoxyl radicals, with absorption maxima at 390 and 410 nm. A major part of these adduct radicals was found to undergo water elimination, leading to phenoxyl radicals, and the process was catalyzed by OH^- (or Na_2HPO_4). The rate of reaction of $\text{O}^{\bullet-}$ with thymol was found to be comparatively low ($k = 1.1 \times 10^9 \text{ dm}^3 \text{ mol}^{-1} \text{ s}^{-1}$), producing H abstracted species of thymol as well as phenoxyl radicals. Further, these phenoxyl radicals of thymol were found to be repaired by ascorbate ($k = 2.1 \times 10^8 \text{ dm}^3 \text{ mol}^{-1} \text{ s}^{-1}$). To support the interpretation of the experimental results, DFT calculations were carried out. The transients (both adducts and H abstracted species) have been optimized in gas phase at B3LYP/6-31+G(d,p) level of calculation. The relative energy values and thermodynamic stability suggests that the ortho adduct ($\text{C}_6\text{-OH}$ adduct) to be most stable in the reaction of thymol with OH radicals, which favors the water elimination. However, theoretical calculations showed that C4 atom in thymol (para position) can also be the reaction center as it is the main contributor of HOMO. The absorption maxima (λ_{max}) calculated from time-dependent density functional theory (TDDFT) for these transient species were close to those obtained experimentally. Finally, the redox potential value of thymol^{*}/thymol couple (0.98 V vs NHE) obtained by cyclic voltammetry is less than those of physiologically important oxidants, which reveals the antioxidant capacity of thymol, by scavenging these oxidants. The repair of the phenoxyl radicals of thymol with ascorbate together with the redox potential value makes it a potent antioxidant with minimum pro-oxidant effects.



1. INTRODUCTION

Studies on natural antioxidants and their role in human health and drug design are subjects of general interest of the past several decades.¹ The majority of the antioxidants comprise phenolic compounds that can scavenge reactive oxygen species and reactive nitrogen species. These reactive species are generated in the biological systems as a result of exposure to ionizing radiations, photosensitization, enzymatic, and biochemical processes. These oxidizing species have a deleterious effect on living cells, mainly on their interaction with DNA, which may lead to diseases like cancer, tumors, and arthritis and also to aging. Of the various reactive free radicals, the OH radical is considered one of the most devastating free radicals and is among the major reactive oxygen species generated during exposure to radiation. The importance of any antioxidant is that it has a sacrificial role in scavenging highly reactive free radicals. Both natural and synthetic antioxidants are generally known to scavenge free radicals. However, synthetic phenolic antioxidants, such as butylated hydroxyanisole and butylated hydroxytoluene, are not advisable, as they have an adverse effect on the human

body.² Thus, natural antioxidants as a safe alternative to synthetic antioxidants are always of interest. In this context, phenolic antioxidants have high importance in the antioxidant series. Thymol (2-isopropyl-5-methylphenol) is a phenolic antioxidant with high relevance in the free radical scavenging processes and it is the compound of interest in the present study.

Thymol is a colorless crystalline monoterpene phenol generally isolated from medicinal plants such as *Thymus vulgaris* and *Oroganum vulgare*.^{3–7} It has a pleasant aromatic odor and is slightly soluble in water at ambient pH. It can be considered a derivative of cymene, containing one phenolic hydroxyl group (OH), one methyl group, and one isopropyl group. Thymol possesses antimicrobial, antifungal, and antioxidant properties and is a major component of the oils of thyme.⁸ These properties are attributed to the presence of the phenolic hydroxyl group in its structure, as phenolic compounds are known to show potent

Received: August 18, 2012

Revised: December 13, 2012

Published: December 14, 2012

antioxidant activity by absorbing and neutralizing free radicals that are harmful to biomolecules.^{9,10} The use of thymol dates back to the ancient Egyptians, in conjunction with its isomer, carvacrol, for the preservation of mummies. It is also used as an active ingredient in food flavorings, perfumes, cosmetics, mouthwash, and a number of oils and topical ointments that have been formulated for massaging the joints and to treat nail fungi. According to the EPA (Environmental Protection Agency), there are no known adverse effects of the use of thymol when used in animals and humans.¹¹

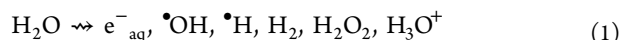
In an earlier free radical study, thymol is reported to be a good scavenger of peroxy radicals (CCl_3O_2 ; calculated rate constants $>10^6 \text{ dm}^3 \text{ mol}^{-1} \text{ s}^{-1}$) with less prooxidant effects.¹² In this study, a detailed investigation is carried out to understand the reaction of OH radicals with thymol using the pulse radiolytic technique. In addition to OH radicals, reactions of azide radical (N_3^\bullet) and oxide radical anion ($\text{O}^{\bullet-}$) have been carried out for a better understanding of the reaction mechanism. The redox potential of thymol has been measured using cyclic voltammetry to support its radical scavenging capacity. Furthermore, to interpret the experimental results computational calculations using Gaussian program were also carried out. By and large, a complete oxidative radical chemistry is investigated with the help of both experimental and theoretical studies.

2. EXPERIMENTAL SECTION

2.1. Chemicals. Thymol (99.5%) was from Sigma-Aldrich. Commercially available sodium azide and 2,2'-azino bis(3-ethylbenzothiazoline-6-sulfonate) (ABTS²⁻), were purchased from Aldrich and were used without further purification. All the reactions were carried out in aqueous medium. Solutions were prepared in water from Millipore A-10 system having conductivity less than $0.1 \mu\text{S/cm}$.

Thymol is reported to aggregate in aqueous medium having a critical micellar concentration of $4 \mu \text{ mol dm}^{-3}$.¹³ Therefore, UV-vis spectra were recorded at varying concentrations of thymol ($0.12\text{--}500 \mu\text{mol dm}^{-3}$) with and without the presence of phosphate buffer (see Supporting Information). However, we did not observe any significant change in the spectral properties and hence the indication of aggregation under our experimental conditions (i.e., in pure aqueous medium).

2.2. Pulse Radiolysis. Radiolysis of water produces three major radical species e_{aq}^- , $\bullet\text{OH}$, $\bullet\text{H}$, along with less reactive H_2 and H_2O_2 .



Pulse radiolysis experiments were carried out using a linear accelerator delivering electron pulse of 7 MeV energy of 50 ns duration. An aerated aqueous solution of KSCN ($1 \times 10^{-2} \text{ mol dm}^{-3}$) was used to monitor the dose per pulse using a $G\mathcal{E}$ value of $2.6 \times 10^{-4} \text{ m}^2 \text{ J}^{-1}$ for $(\text{SCN})_2^{\bullet-}$ at 475 nm,¹⁴ and the dose was kept at 13.5 Gy. The details of pulse radiolysis setup have been described elsewhere.¹⁵

To study the reaction of thymol with OH radicals, e_{aq}^- formed in the radiolysis were converted to OH radical by saturating the solution with N_2O .

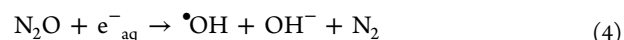
The specific one-electron oxidant N_3^\bullet radical was produced in N_2O saturated solution containing $0.02 \text{ mol dm}^{-3} \text{ NaN}_3$.



In basic conditions, the H^\bullet is converted to e_{aq}^- with a rate constant of $2.2 \times 10^7 \text{ dm}^3 \text{ mol}^{-1} \text{ s}^{-1}$, according to eq 3.



On saturating the solution with N_2O at high pH, e_{aq}^- is quantitatively converted to $\text{O}^{\bullet-}$, because $\bullet\text{OH}$ is in equilibrium with $\text{O}^{\bullet-}$ at high pH ($\bullet\text{OH} \rightleftharpoons \text{O}^{\bullet-}$; $pK_a = 11.9$)



The bimolecular rate constant values were determined from the rate of buildup of transients (pseudounimolecular) under varying concentrations of thymol.

2.3. Computational Method. Density functional theory calculations were performed on the Gaussian 03 computational package.¹⁶ As Becke's three-parameter hybrid functional combined with correlation functional of Lee, Yang, and Parr, denoted as B3LYP¹⁷ has been effective for obtaining the optimal geometries, harmonic frequencies, and electronic properties, a similar procedure is followed for the present study. All the geometries were optimized without any symmetry constraints, with the 6-31+G(d,p) basis set, in gas phase. Spin unrestricted calculations were performed for open shell systems. Optimized structures were identified as local minima with real harmonic vibrational frequencies and the saddle point with one imaginary frequency. TDDFT method was used to calculate the excited state electronic properties.¹⁸

2.4. Cyclic Voltammetry. The cyclic voltammetric experiments were carried out using an Autolab Electrochemical System (Eco Chemie, The Netherlands), PGSTAT 20 driven by GPES software. Platinum wire of about 1 mm diameter was used as working and counter electrode. The reference electrode used was Ag/AgCl, 3 M KCl electrode. Working and counter electrodes were thoroughly cleaned before each measurement. Blank measurements were also carried out before each scan. Solutions were deaerated by bubbling N_2 for 10 min prior to recording the cyclic voltammogram.

3. RESULTS AND DISCUSSION

3.1. Reaction with OH Radicals. a. Pulse Radiolysis Studies. Reaction of OH radicals with thymol was carried out at pHs 5.8, 7.8, and 9.2, where thymol exists in its neutral form. A bimolecular rate constant of $8.1 \times 10^9 \text{ dm}^3 \text{ mol}^{-1} \text{ s}^{-1}$ was determined from the pseudo-first-order buildup of the transient at 340 nm as a function of thymol concentration at pH 5.8 (Table 1). The dependence of the pseudo-first-order rate constant

Table 1. Absorption Maxima of the Transients and Second-Order Rate Constants for the Reaction of Thymol with Selected Oxidizing Radicals

radicals	pH	λ_{max} (nm)	k_2 ($\text{dm}^3 \text{ mol}^{-1} \text{ s}^{-1}$)
$\bullet\text{OH}$	5.8	330	8.1×10^9
$\text{O}^{\bullet-}$	>13.5	330, 390, 410	1.1×10^9
N_3^\bullet	6.8	390, 410	2.3×10^9

against the concentration of thymol is presented in the Supporting Information. The transient spectrum recorded at 2 μs after the pulse at pH 5.8 has a maximum at 330 nm (Figure 1). This was found to undergo decay with respect to time. A small hike in the spectrum at around 400 nm region (390 and 410 nm) is also observed when the spectrum was recorded at 40 μs after the pulse. Although the absorbance is very feeble at this region, it was highly reproducible. When the spectrum was recorded at pH

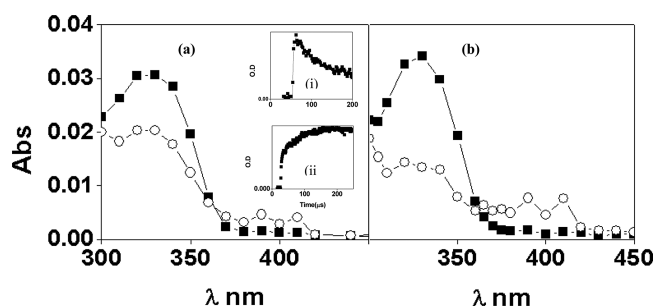


Figure 1. Time-resolved absorption spectra obtained by pulse radiolysis of N_2O saturated $5 \times 10^{-4} \text{ mol dm}^{-3}$ thymol solution at (a) pH 5.8 and (b) pH 7.8 at (■) $2 \mu\text{s}$ and (○) $40 \mu\text{s}$ after the electron pulse. Insets: (i) Decay traces at 340 nm at pH 5.8. (ii) Absorption buildup of $\text{ABTS}^{\bullet-}$ at 735 nm.

7.8, the absorption buildup was more prominent at 400 nm region (Figure 1). A similar trend was observed even at pH 9.2. At pH 9.2 the transient absorption at 330 nm fully decayed after $20 \mu\text{s}$ (spectrum not shown).

The absorption traces at 330 nm obtained at pH 5.8 and 7.8 showed that the decay rate of the transient at 330 nm followed first-order kinetics and was found to increase with pH ($k_{\text{p}} = 1.09 \times 10^4 \text{ s}^{-1}$ at pH 5.8 and $k_{\text{p}} = 2.9 \times 10^4 \text{ s}^{-1}$ at pH 7.8). The decay was also monitored in the presence of Na_2HPO_4 and a significant increase in the rate of decay is observed. Because the rate of decay at 330 nm was found to increase with an increase in the concentration of Na_2HPO_4 (Figure 2), it is clear that the rate of transformation can also be enhanced by phosphate

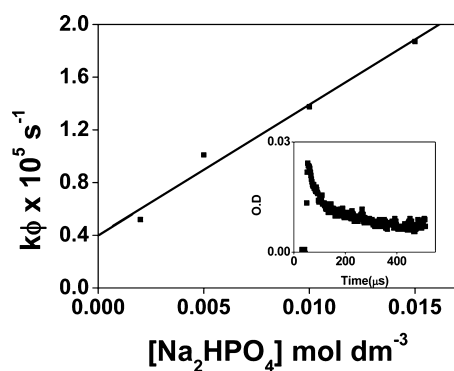


Figure 2. Dependence of the decay kinetics of the intermediate with respect to the concentration of Na_2HPO_4 in the reaction of $\bullet\text{OH}$ with thymol ($5 \times 10^{-4} \text{ mol dm}^{-3}$) at 330 nm. Inset: decay at 330 nm without buffer.

To study the redox property of the transients, reactions were carried out in the presence of ABTS^{2-} , at sufficiently low concentrations at pH 5.8 so as to avoid direct reaction of OH radicals with the reductant. A clear absorption buildup of $\text{ABTS}^{\bullet-}$ was monitored at 735 nm (Figure 1). This clear absorption buildup of $\text{ABTS}^{\bullet-}$ indicated the presence of an oxidizing intermediate, as it is well-known that the one-electron oxidation of ABTS^{2-} by the oxidizing radicals generates $\text{ABTS}^{\bullet-}$ absorbing at 735 nm.¹⁹

The reaction of azide radical (N_3^{\bullet}) with thymol has been carried out at pH 6.8. The time-resolved transient absorption spectrum obtained from the reaction of N_3^{\bullet} with thymol is shown in Figure 3. A reaction rate constant of $2.3 \times 10^9 \text{ dm}^3 \text{ mol}^{-1} \text{ s}^{-1}$ has also been determined. The transient spectrum showed two clear absorption maxima at 390 and 410 nm. The

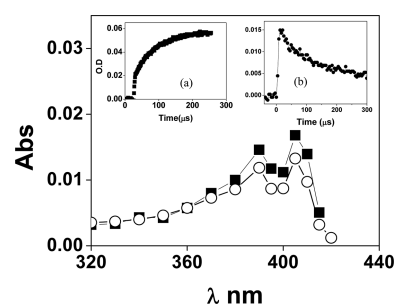
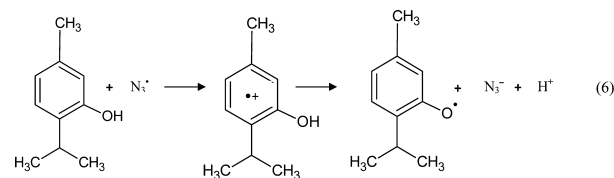


Figure 3. Time-resolved transient absorption spectra obtained by pulse radiolysis of N_2O -saturated aqueous solution containing 0.01 mol dm^{-3} NaN_3 and $5 \times 10^{-4} \text{ mol dm}^{-3}$ thymol solution at pH 6.8 after (■) $2 \mu\text{s}$ and (○) $40 \mu\text{s}$ after the electron pulse. Insets: (a) absorption buildup of $\text{ABTS}^{\bullet-}$ at 735 nm obtained from the reaction of intermediate with ABTS^{2-} at pH 6.8; (b) decay of phenoxyl radical of thymol at 410 nm obtained by the reaction of $5 \times 10^{-4} \text{ mol dm}^{-3}$ thymol with $\bullet\text{N}_3$ at pH 6.8 (very similar decay trace was obtained in the presence of $\text{N}_2\text{O}:\text{O}_2 = 4:1$).

oxidizing nature of the intermediate radical is demonstrated from the reaction of ABTS^{2-} . The absorption buildup obtained at 735 nm (Figure 3) confirms the formation of an oxidizing radical of thymol.

Azide radical is a known specific one-electron oxidant²⁰ ($E_0 = 1.33 \text{ V vs NHE}$). This radical is generally known to produce a radical cation of both heterocyclic and homocyclic compounds.²¹ It is reported that a phenolic type radical can be formed from the reaction of azide radical with organic compounds containing phenolic moiety.^{22,23} In this context, it is very likely that the azide radical produces a phenoxyl radical potentially formed from the result of deprotonation of the initially formed radical cation (reaction 6). The oxygen-centered radical can be convincingly an oxidizing radical that can easily react with ABTS^{2-} . A similar oxidizing nature for oxygen-centered radical is reported.^{24–26} The oxidizing property of this intermediate was further confirmed in the presence of oxygen. A typical absorption decay at 410 nm in the presence of 20% oxygen was investigated. A very similar decay pattern at 410 nm was observed in the absence and presence of oxygen, which clearly indicates the oxidizing nature of the intermediate and hence the assignment as phenoxyl radical.

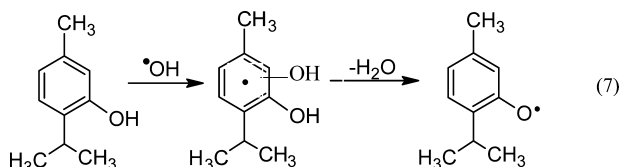


As it is presumed that only the phenoxyl radical is formed from the reaction of azide radical with thymol, the yield of $\text{ABTS}^{\bullet-}$ is taken as 100%. Based on this assumption, the yield of $\text{ABTS}^{\bullet-}$ in the case of the reaction of OH radical is calculated as $0.22 \mu\text{mol J}^{-1}$ at pH 5.8, which constitutes nearly 35% of the total reaction.

On comparison of the spectrum obtained with azide radicals (Figure 3) with that of the OH radical (Figure 1a,b), it is possible to assign the absorption maxima at 390 and 410 nm to the phenoxyl radical in both the reactions. Thus, the absorption at 390 and 410 nm observed in the case of the reaction of OH radicals is an indication of the formation of the phenoxyl type radical of thymol, though in a low yield (Figure 1). A close analysis of the spectrum (Figure 1) at longer time scale shows a

buildup of the absorbance at 390 and 410 nm with a concomitant decay at 330 nm.

On the other hand, the reaction of OH radical with thymol resulted an absorption spectrum with a predominant species having a maximum at 330 nm in the initial stage. One of the major possibilities of $\cdot\text{OH}$ attack is in the benzene ring itself with a characteristic absorption in the 310–350 nm range.^{22,23,27–32} It is well-known that OH radicals add to benzene ring systems to form cyclohexadienyl type radicals.^{21,22,27} It is therefore highly likely that the initial species with 330 nm is the OH-adduct of thymol. The decay at the 330 nm can be understood as the dehydration of the OH-adduct to produce the stable phenoxyl radical of thymol (reaction 7).



Thus probable mechanism of the reaction of OH radicals with thymol, involves the initial formation of an OH₂ adduct, which then undergoes a water elimination reaction catalyzed by OH⁻ (or Na₂HPO₄) leading to a phenoxyl radical. On the other hand, the yield of phenoxyl radical, as obtained from the yield of ABTS^{•-}, is only about 35%, which indicates that there could be other intermediates formed under this conditions. It is understandable that only those additions which are adjacent to the -OH group can favor water elimination. It is very probable that $\cdot\text{OH}$ can attack in other positions as well. As these individual adduct isomers are closely related to their physical and chemical properties, it is a difficult task to identify these isomers from their spectral behavior. Computational methods have been proven effective for predicting the probable reaction mechanisms involving radical species.^{33,34} To resolve the existence of the various adduct radicals and to clearly identify the structure and the reaction possibilities, we have carried out a detailed DFT calculation and the results obtained are discussed and compared with the experimental findings.

b. Theoretical Study on the Reaction of OH Radicals.

i. Structure and Electronic Properties of Thymol. The optimized geometry of thymol in the gas phase is depicted in the Figure 4 with the important bond lengths in Å.

From the Figure 4 we can see that the bond lengths C1–C6, C2–C3, and C4–C5 are 1.395, 1.398, and 1.398 Å, respectively. Of these, the shortest bond distance is between C1 and C6, suggesting a more double bond character. This may be attributed to the presence of the phenolic group; otherwise, the bond lengths would be the same due to the equal distribution of the π electron cloud over the aromatic ring. Because more double bond character is observed in the C1–C6 bond, constituent atoms of this bond are expected to be more reactive sites for an electrophilic addition reaction with the hydroxyl radical.

The molecular electrostatic potential (MESP) is a useful tool to predict the reaction center, by locating the electron rich center at the most negative valued atoms (V_{min}).³⁵ The MESP analysis showed the most negative values of -0.402937, -0.308019, and -0.169601 for C2, C6, and C4 atoms, respectively. The MESP plot is shown in Figure 5. These values suggest that C2, C6, and C4 atoms are the potential centers for the electrophilic attack of the OH radical.

ii. Addition Reactions of OH Radical with Thymol. We have initially considered the possibility of the addition of the OH

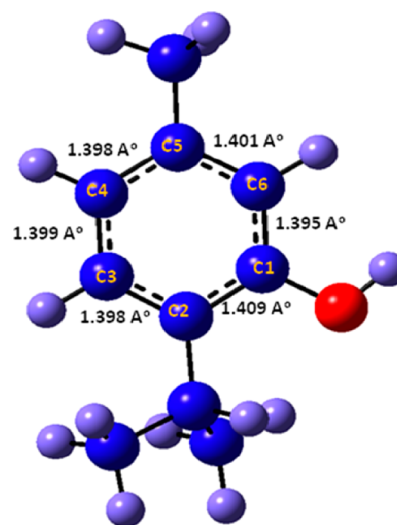


Figure 4. Optimized geometry of thymol at the B3LYP/6-31+G(d,p) level of theory. Bond lengths are in Å.

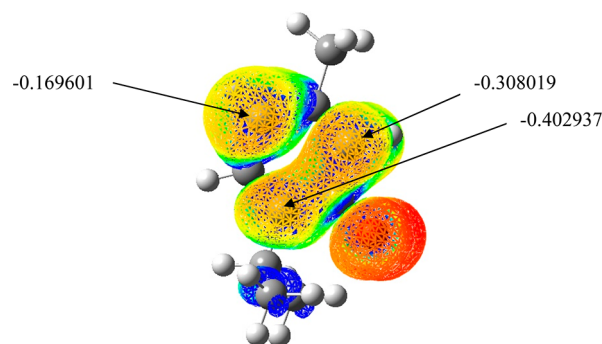


Figure 5. MESP (V_{min}) located near the C2, C6, and C4 atoms.

radical to all five sites of the aromatic ring (Scheme 1). The adducts thus formed, viz. C2_{OH}, C3_{OH}, C4_{OH}, C5_{OH}, and C6_{OH}, have been modeled and optimized. The optimized geometries of the adduct radicals are depicted in Figure 6. Also, their relative energy values with respect to the sum of the energies of the thymol molecule and the OH radical are shown. For the C2_{OH} adduct, the spin maxima are centered on the C5, C1, and C3 atoms and the values are 0.58, 0.49 and 0.35, respectively. For the C6_{OH} adduct, the spin maxima are on the C3, C5, and C1 atoms and the values obtained are 0.6, 0.5, and 0.4 respectively. These correspond to the resonance forms of the thymol $\cdot\text{OH}$ adduct radical systems.

According to the relative energy values, the order of stability of the OH adduct of thymol, computed in the gas phase is C6_{OH} adduct > C2_{OH} adduct > C4_{OH} adduct. The relative enthalpies as well as the relative free energy values of these radical adducts also show the same trend as that of their relative energy values (Figure 7). Furthermore, the relative enthalpies, relative free energy values and the relative energy of these radical adduct systems also agrees with the MESP analysis, as it shows V_{min} at C2, C4, and C6 (Figure 5).

In addition, we have considered the possibility of the formation of an intermediate complex between the thymol ground state and the OH radical. For this we optimized the structure of an intermediate in which the oxygen of the OH radical pointed toward the π -face of the thymol. It is found that the OH radical moved out from the π -face to the plane of the

Scheme 1. Possible Addition Reactions of Hydroxyl Radicals with Thymol

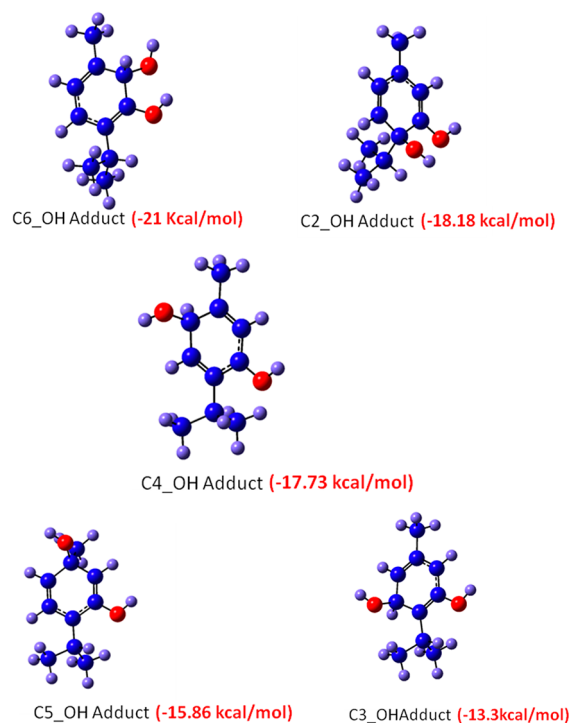
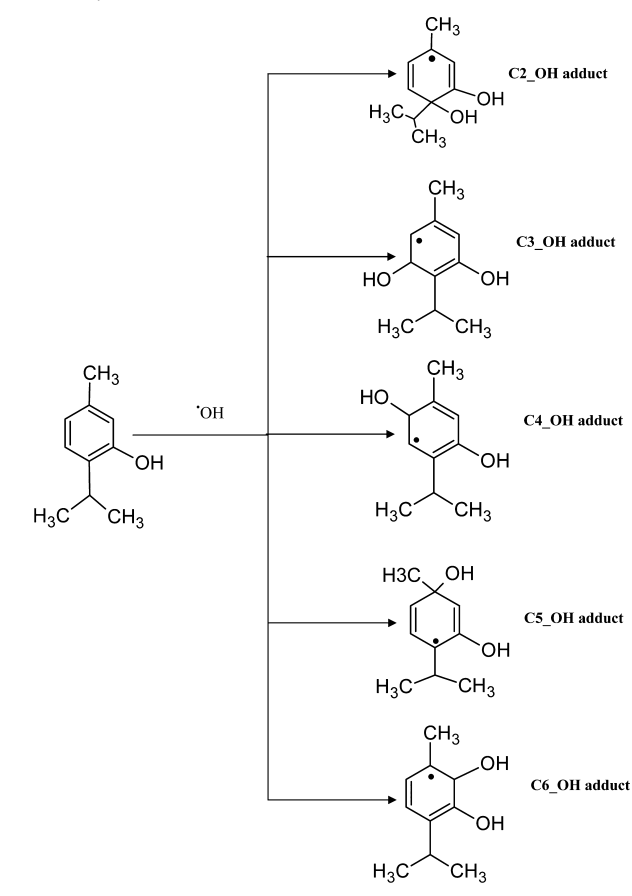


Figure 6. Optimized structures of the adducts, in gas phase, at the B3LYP/6-31+G(d,p) level of theory. The relative energy is shown in parentheses.

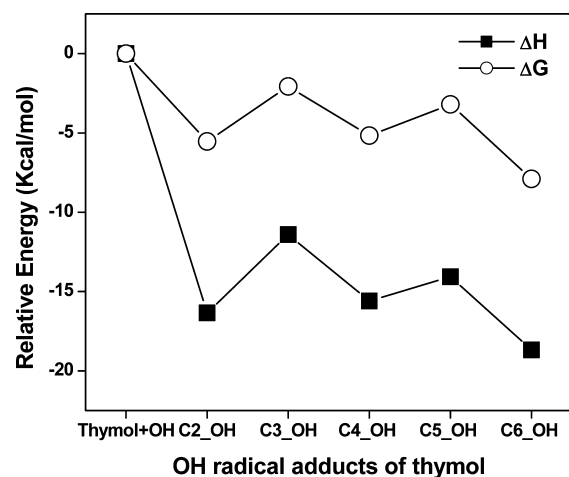
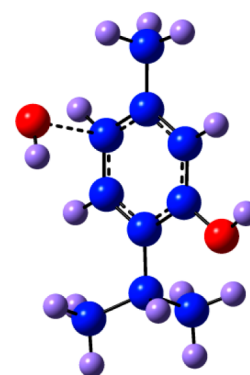


Figure 7. Relative enthalpy change (ΔH) and free energy change (ΔG) for the OH addition reactions computed, in gas phase, at the B3LYP/6-31+G(d,p) level of theory.

molecule and eventually forming a reaction-complex [thymo- \cdots OH] presented in Figure 8. In this complex, the oxygen of OH



[Thymol...OH]

Figure 8. Complex formed as a result of OH reaction of thymol, optimized at the B3LYP/6-31+G(d,p) level.

radical is at a distance of 2.26 Å from C4 atom of thymol and the relative energy of this complex is -6.8 kcal/mol. The activation energy required for the formation of the C4_OH adduct from this complex is found to be of 0.08 kcal/mol (Scheme 2). The highest occupied molecular orbital (HOMO) of thymol (Figure 9) shows high MO coefficient at C4 atom which favors the electrophilic addition of the OH radical at this center. This further supports the addition of OH radical at C4 atom as one of the potential reaction channels.

Because the C4_OH adduct formation takes place by a barrierless reaction, the adduct formation reactions is expected to be a spontaneous reaction leading to a direct addition of hydroxyl radical to thymol. However, unlike the C4_OH adduct, the two OH groups in the thermodynamically stable, C2_OH and C6_OH adducts, are in adjacent positions favoring the elimination of water, thus yielding the phenoxyl radical of thymol. The C4_OH adduct is presumed to undergo radical-radical decay and gives rise to stable end products.

iii. *TDDFT Calculations.* The optical absorption maxima (λ_{\max}) for the thermodynamically stable C2_OH and C6_OH

Scheme 2. Representation of the Formation of the C4_OH Adduct from the Complex S1 via a Transition State (TS), Which Has Very Low Barrier Energy

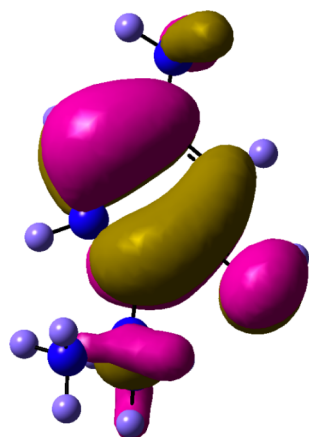
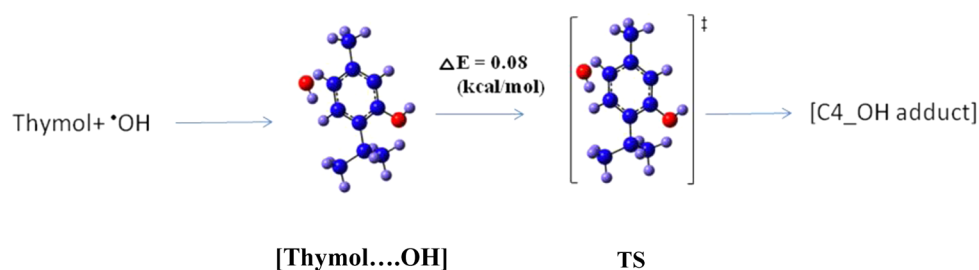


Figure 9. Highest occupied molecular orbital of thymol calculated at the B3LYP/6-31+G(d,p) level of calculation.

adducts were calculated using TDDFT method and values of 339.11 and 342.11 nm were observed, in the gas phase. The TDDFT calculation at the same level for the kinetically favored C4_OH adduct showed a transition wavelength (absorption maximum) of 332.04 nm. These values are close to the experimentally observed λ_{max} of 330 nm. Though the TDDFT calculation supports the existence of the above adducts, the thermodynamic considerations prefers C6_OH adduct to C4_OH adduct and the kinetic consideration favors C4_OH adduct. From the above studies, it is clear that OH radical attacks thymol, at the ortho (preferably at C6) position to yield adducts that are thermodynamically more stable than that formed by the attack at the para (C4) position of the phenolic group. The experimental results are in line with this observation as both water eliminated species and the stable (at the pulse radiolysis scale) OH-adduct contribute to the observed spectrum.

3.2. Reaction of $\text{O}^{\bullet-}$ with Thymol. a. Pulse Radiolysis. The reaction of oxide radical anion with thymol has been carried out at pH ~ 14 . The absorption spectrum obtained for the transient species as a result of $\text{O}^{\bullet-}$ reaction with thymol, recorded at 2 and 40 μs after the electron pulse (Figure 10), is characterized by absorption maxima at 330, 390, and 410 nm. As the pK_a of thymol is determined to be 10.45, the deprotonated form (anionic form) of thymol is the species that reacts with $\text{O}^{\bullet-}$ radicals. The bimolecular rate constant for the reaction of $\text{O}^{\bullet-}$ radical was determined by following the buildup of the transient absorption at 390 nm as a function of thymol concentration and is given in Table 1.

The oxidizing property of the transients was monitored by its reaction with the reductant, ABTS^{2-} , by monitoring the absorption buildup at 735 nm, which corresponds to the one-

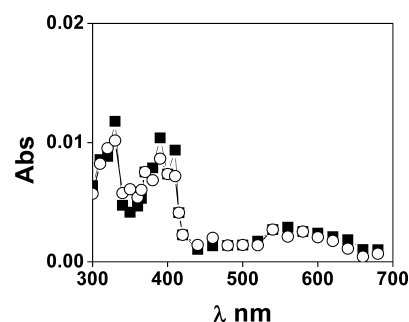


Figure 10. Time-resolved transient absorption spectra obtained by pulse radiolysis of N_2O -saturated $5 \times 10^{-4} \text{ mol dm}^{-3}$ thymol solution at pH ~ 14 at (■) 2 μs and (○) 40 μs after the electron pulse.

electron oxidized species, $\text{ABTS}^{\bullet-}$. A bimolecular rate constant of $4 \times 10^8 \text{ dm}^3 \text{ mol}^{-1} \text{ s}^{-1}$ was also calculated for the reaction. This value is almost the same as that obtained with the intermediate formed in the azide radical reaction.

The oxide radical anion ($\text{O}^{\bullet-}$) is known to react by one-electron oxidation. Hence it reacts with the monoanionic form of thymol by one-electron oxidation mainly from the anionic center located at the oxygen atom, leading to the production of the oxygen-centered phenoxyl radical. From the earlier discussions, the peaks at 390 and 410 nm were identified as that of the phenoxyl radicals. These phenoxyl radicals are mostly oxidizing in nature. The yield of the oxidizing radicals was calculated to be 62.8% of the total radical reaction (assuming that the yield of $\text{O}^{\bullet-}$ is $0.6 \mu\text{mol J}^{-1}$).

However, the reaction of thymol anion with $\text{O}^{\bullet-}$ radicals can also proceed via H-abstraction mostly from the $-\text{HC}(\text{CH}_3)_2$ and/or $-\text{CH}_3$ groups. Both these reactions lead to the production of carbon-centered radicals, which are reducing in nature. As addition of $\text{O}^{\bullet-}$ radicals to the aromatic ring is not a common reaction, it is likely that $\text{O}^{\bullet-}$ radicals undergo H-abstraction reactions and the peak at 330 nm has been assigned to these H-abstracted species. H-abstraction reaction of $\text{O}^{\bullet-}$ is already reported in a number of compounds.³⁶

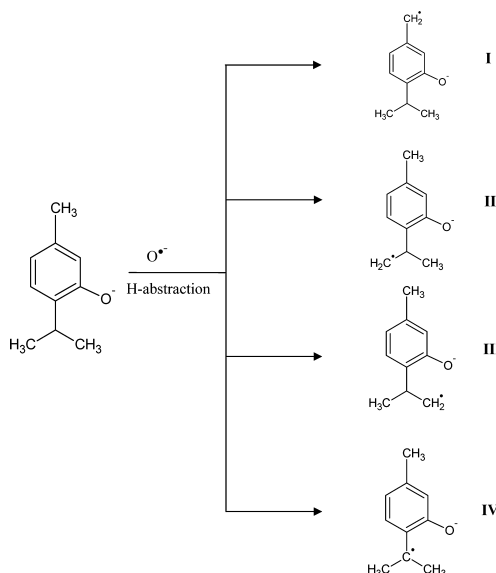
Thus, it is clear that the reaction of $\text{O}^{\bullet-}$ radicals with thymol produces a mixture of oxidizing and reducing radicals. To distinguish the two major reaction pathways such as electron transfer and H-abstraction reaction as well as the various H-abstracted species, we have carried out DFT calculations as in the case of the reaction of OH radicals.

b. Theoretical Study on the Reaction of $\text{O}^{\bullet-}$ Radicals. The oxide radical anion ($\text{O}^{\bullet-}$) is known to undergo one-electron oxidation as well as H-abstraction reactions, compared to addition reactions, and in this study we have presented the reaction possibilities of H-abstraction reactions as well as one-

electron oxidation reaction from the monoanionic form of thymol.

i. H-Abstraction Reactions of $O^{\bullet-}$ with Thymol. The H-abstraction reactions occur mainly from the methyl and isopropyl substituents of the monoanionic form of thymol. The H-abstraction results in the carbon-centered radicals and the various possible radicals are depicted in the Scheme 3. The radicals are

Scheme 3. Possible H-Abstracted Species Formed from the Reaction of the $O^{\bullet-}$ Radical

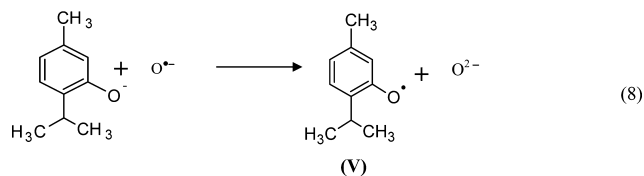


optimized at the B3LYP/6-31+G(d,p) level of calculation. The relative energies of these radicals (with respect to the least stable radical species) are shown in Table 2. From the table it is clear that both the relative energy values and relative free energy values shows the same trend.

Table 2. B3LYP/6-31+G(d,p)-Calculated (in the Gas Phase) Relative Energy Changes of the Various Possible Radicals with the Reaction of $O^{\bullet-}$ with Thymol

radical species	enthalpy change (ΔH , kcal/mol)	free energy change (ΔG , kcal/mol)
I	-12.8	-10.7
II	0.00	0.00
III	-0.07	-0.25
IV	-16.4	-16.3
V	-372	-361.25

ii. One-Electron Oxidation of $O^{\bullet-}$ with Thymol. The oxide radical anion is known to undergo one-electron oxidation, as shown in eq 8.



The radical resulting from one-electron oxidation is the oxygen-centered radical (V). This radical is also optimized as in the case of carbon-centered radicals, and the relative energy is compared with that of the least stable carbon-centered radical. It

is found that this oxygen-centered radical is the most stable one (with a relative energy of $-361.25 \text{ kcal mol}^{-1}$) in the gas phase. Thus the above thermodynamic considerations show that the oxygen-centered radical is the most stable radical when compared to the carbon-centered radicals formed by the H-abstraction reactions. The probable carbon-centered radicals formed are mainly IV/I.

These theoretical studies are in line with the experimental results, which showed a maximum yield of phenoxy type radical as the major transient and the carbon-centered radicals as the minor transient.

3.3. Scavenging of the Phenoxy Radical of Thymol by Ascorbate Ions. The phenoxy radical formed from the above-described oxidation reactions might in turn attack proteins, lipids, and other delicate molecules like DNA. Thus in this context it is relevant to study the scavenging of phenoxy radicals with endogenous antioxidant. Vitamin C (ascorbic acid) is an endogenous water-soluble physiological antioxidant. It has a pK_a at 4.1 and 11.8 and therefore it exists as a monoanion ($AscH^-$) at neutral pH.³⁷ The one-electron oxidized species of $AscH$ is characterized by the absorption maximum at 360 nm ($\epsilon = 3300 \text{ dm}^3 \text{ mol}^{-1} \text{ cm}^{-1}$).³⁸ The experiment was performed with $2 \times 10^{-3} \text{ mol dm}^{-3}$ of thymol with varying concentrations of ascorbic acid [$(0.1-0.06) \times 10^{-3} \text{ mol dm}^{-3}$]. It was observed that in the presence of ascorbic acid, the decay of the phenoxy radicals of thymol was much faster than in its absence. Also it is found that there is a simultaneous absorption buildup at 360 nm.

Typical traces that were obtained from the pulse radiolysis of N_2O saturated $2 \times 10^{-3} \text{ mol dm}^{-3}$ thymol containing $1 \times 10^{-4} \text{ mol dm}^{-3}$ ascorbic acid and $0.01 \text{ mol dm}^{-3} NaN_3$ are given in Figure 11. This suggests that the phenoxy radicals of thymol,

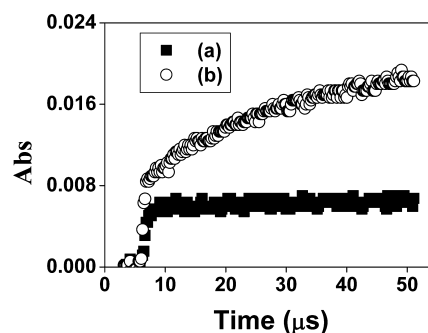
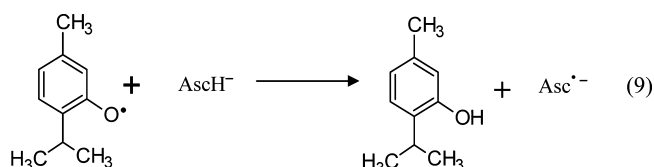


Figure 11. Absorption traces obtained on pulse radiolysis of N_2O saturated $2 \times 10^{-3} \text{ mol dm}^{-3}$ thymol solution containing $1 \times 10^{-4} \text{ mol dm}^{-3}$ ascorbic acid and $0.01 \text{ mol dm}^{-3} NaN_3$. (a) Absorption trace at 360 nm in the absence of ascorbic acid. (b) Formation of ascorbate radical anion at 360 nm in the presence of $1 \times 10^{-4} \text{ mol dm}^{-3}$ ascorbic acid.

which are oxidizing, are scavenged by the ascorbic acid anion, giving ascorbate anion radical (eq 9). The rate constant for this reaction was determined by following the pseudo-first-order buildup at 340 nm as $2.1 \times 10^8 \text{ dm}^3 \text{ mol}^{-1} \text{ s}^{-1}$.



This high value of the rate constant indicates that the phenoxy radicals of thymol can be efficiently scavenged by the ascorbic

V.; Nolan, M. V.; Zygadlo, J. A.; Perillo, M. A. *Biophys. Chem.* **2006**, *122*, 101–113.

(14) Buxton, G. V.; Stuart, C. R. *J. Chem. Soc., Faraday Trans.* **1995**, *91*, 279–281.

(15) Guha, S. N.; Kishore, K.; Moorthy, P. N.; Naik, D. B.; Rao, K. N. *Proc. Indian Acad. Sci. (Chem. Sci.)* **1987**, *99*, 261–271.

(16) Frisch, M. J.; Trucks, G. W.; Schlegel, H. B.; Scuseria, G. E.; Robb, M. A.; Cheeseman, J. R.; Montgomery, J. A.; Vreven, T.; Kudin, K. N.; Burant, J. C.; et al. *Gaussian 03*, Revision C.02s; Gaussian, Inc.; Wallingford, CT, 2004.

(17) (a) Becke, A. D. *J. Chem. Phys.* **1993**, *98*, 5648. (b) Lee, C.; Yang, W.; Parr, R. G. *Phys. Rev. B* **1988**, *37*, 785.

(18) Stratmann, R. E.; Scuseria, G. E.; Frisch, M. J. *J. Chem. Phys.* **1998**, *109*, 8218–8224.

(19) von Sonntag, C. *The chemical Basis of Radiation Biology*; Taylor and Francis: London, 1987.

(20) Wardman, P. *J. Phys. Chem. Ref. Data* **1989**, *18*, 1637–1754.

(21) Zeev, B. A.; Schuler, R. H. *J. Phys. Chem.* **1985**, *89*, 3359–3363.

(22) Mohan, H. *Radiat. Phys. Chem.* **1996**, *49*, 15–19.

(23) Bjergbakke, E.; Sillesen, A.; Pagsberg, P. *J. Phys. Chem.* **1996**, *100*, 5729–5736.

(24) Bordwell, F. G.; Cheng, J. P. *J. Am. Chem. Soc.* **1991**, *113*, 1736–1743.

(25) Lind, J.; Shen, X.; Eriksen, T. E.; Merenyi, G. *J. Am. Chem. Soc.* **1990**, *112*, 479–482.

(26) (a) Dhiman, S. B.; Kamat, J. P.; Naik, D. B. *Chem.-Biol. Interact.* **2009**, *182*, 119–127. (b) Priyadarsini, K. I.; Devasagayam, T. P. A.; Rao, M. N. A.; Guha, S. N. *Radiat. Phys. Chem.* **1999**, *54*, 551.

(27) Fang, X.; Pan, X.; Rahmann, A.; Schuchmann, H. P.; Sonntag, C. *V. Chem.—Eur. J.* **1995**, *7*, 423–429.

(28) Spinks, J. W. T.; Woods, R. J. *An Introduction to Radiation chemistry*; Wiley Interscience Publication: New York, 1990.

(29) Ragahavan, N. V.; Steenken, S. *J. Am. Chem. Soc.* **1980**, *102*, 3495–3499.

(30) Solar, S.; Solar, W.; Getoff, N. *J. Phys. Chem.* **1984**, *88*, 2091–2095.

(31) Mvula, E.; Schuchmann, M. N.; von Sonntag, C. *J. Chem. Soc., Perkin Trans. 2* **2001**, 264–268.

(32) Tripathi, G. N. R.; Su, Y. *J. Phys. Chem. A* **2004**, *108*, 3478–3484.

(33) Pramod, G.; PrasanthKumar, K. P.; Mohan, H.; Manoj, V. M.; Manoj, P.; Suresh, C. H.; Aravindakumar, C. T. *J. Phys. Chem. A* **2006**, *110*, 11517–11526.

(34) PrasanthKumar, K. P.; Mohan, H.; Pramod, G.; Suresh, C. H.; Aravindakumar, C. T. *Chem. Phys. Lett.* **2009**, *467*, 381–386.

(35) (a) Politzer, P.; Truhlar, D. G. *Chemical Applications of Atomic and Molecular Electrostatic Potentials*; Plenum: New York, 1981. (b) Gadre, S. R.; Shirsat, R. N. *Electrostatics of Atoms and Molecules*; University Press: Hyderabad, India, 2000. (c) Suresh, C. H.; Gadre, S. R. *J. Org. Chem.* **1999**, *64*, 2505. (d) Suresh, C. H.; Gadre, S. R. *J. Am. Chem. Soc.* **1998**, *120*, 7049.

(36) David, A. A.; Asmus, K. D.; Bonifacic, M. *J. Phys. Chem. A* **2004**, *108* (12), 2238–2246.

(37) Packer, J. E.; Slater, T. F.; Wilson, R. L. *Nature* **1979**, *278*, 737–738.

(38) Schuler, R. H. *Radiat. Res.* **1977**, *69*, 417–433.

(39) (a) Kilmartin, P. A.; Zou, H.; Waterhouse, A. L. *J. Agric. Food Chem.* **2001**, *49*, 1957–1965. (b) Joshi, R.; Gangabhagirathi, R.; Venu, S.; Adhikari, S.; Mukherjee, T. *Free. Radical. Res* **2012**, *46*, 11–20. (c) Pryor, W. A. *Bio-assays for oxidative stress status*; Elsevier Science B.V.: Amsterdam, The Netherlands, 2001.